Original Article

Vortex formation time as an index of left ventricular filling efficiency: comparison between children volunteers and patients with tetralogy of Fallot

Li-Wei Hu[1], Yang Xiang[2], Su-Yang Qin[2], Rong-Zhen Ouyang[1], Jin-Long Liu[3], Ya-Feng Peng[1], Wei-Hui Xie[1], Yong Zhang[4], Hong Liu[2], Yu-Min Zhong[1]

[1]Diagnostic Imaging Center, Shanghai Children's Medical Center Affiliated with Shanghai Jiao Tong University School of Medicine, Shanghai, China; [2]J.C. Wu Center for Aerodynamics, School of Aeronautics and Astronautics, Shanghai Jiao Tong University, Shanghai, China; [3]Department of Cardiovascular and Thoracic Surgery, Shanghai Children's Medical Center Affiliated with Shanghai Jiao Tong University School of Medicine, Shanghai, China; [4]MR Research, GE Healthcare, Shanghai, China

Contributions: (I) Conception and design: LW Hu, YM Zhong; (II) Administrative support: YM Zhong; (III) Provision of study materials or patients: LW Hu, SY Qin, JL Liu; (IV) Collection and assembly of data: LW Hu, RZ Ouyang; (V) Data analysis and interpretation: LW Hu, YF Peng, WH Xie; (VI) Manuscript writing: All authors; (VII) Final approval of manuscript: All authors.

Correspondence to: Yu-Min Zhong. Diagnostic Imaging Center, Shanghai Children's Medical Center Affiliated with Shanghai Jiao Tong University School of Medicine, 1678 Dongfang Road, Shanghai 200127, China. Email: zyumin2002@163.com; Hong Liu. J.C. Wu Center for Aerodynamics, School of Aeronautics and Astronautics, Shanghai Jiao Tong University, 800 Dongchuan Road, Shanghai 200240, China. Email: hongliu@sjtu.edu.cn.

Background: Vortex formation time (VFT) had been considered a useful marker for assessing diastolic performance. the VFT assessment of diastolic function using four-dimensional (4D) flow cardiovascular magnetic resonance (CMR) has not been used in repair of tetralogy of Fallot (rTOF) patient. The aims of this study were as follows: (I) establish reference ranges for VFT measurements in healthy children and adolescents using 4D flow CMR imaging; and (II) analyze VFT parameters to assess diastole dysfunction in rTOF patients group.

Methods: We acquired the CMR data was of 62 healthy participants (aged 6–18 years; male: 40, female: 22) and 20 patients with rTOF (aged 10–13 years; male: 15, female: 5) using 4D flow and cine sequence in routine chamber view. The VFT was calculated based on comparison of different algorithms from cine measurements (VFT_{volume}) and 4D flow measurements (VFT_{blood}). Then, VFT measurements were compared to subject peak filling rate (PFR), age, and cardiac mass using simple linear regression and multiple regression analyses. Data were also categorized according to age for VFT and cardiac functional assessment comparisons between 3 age groups (Group 1: 6–9 years; Group 2: 10–13 years; Group 3: 14–18 years). The correlation of VFT and cardiac function parameters were analyzed in the rTOF group.

Results: Normal mean value of VFT_{volume} and VFT_{blood} were 4.25±0.92 and 3.77±1.11 in healthy children participants. The VFT_{volume} was correlated with VFT_{blood} (r=0.61, P<0.001). There was a moderately significant correlation between VFT_{volume} and PFR (r=0.46, P<0.001) and between VFT_{blood} and PFR (r=0.47, P<0.001), age (r=0.41, P=0.002) and left ventricular (LV) mass (r=0.48, P<0.001). Multiple regression analyses demonstrated that VFT_{volume} was independently associated with PFR (T=2.239; P<0.05) and VFT_{blood} (T=4.361; P<0.001). There was a significant difference in VFT_{volume} between healthy controls and rTOF patients (5.44±1.93 *vs.* 4.27±0.88, P=0.018).

Conclusions: The VFT measurements showed that the LV that had appropriate space to form the optimal vortex ring in normal children and adolescents aged 6–18 years old. The VFT_{volume} could potentially be helpful in improving our understanding of LV diastolic dysfunction in rTOF patients.

Keywords: Cardiovascular magnetic resonance (CMR); 4D flow; vortex formation time (VFT); vortex flow; intracardiac blood flow patterns

Submitted Feb 11, 2022. Accepted for publication Apr 02, 2022.
doi: 10.21037/tp-22-67
View this article at: https://dx.doi.org/10.21037/tp-22-67

Introduction

Vortex formation time (VFT), as originally defined by Gharib *et al.*, has been applied as an important index to characterize propulsion efficiency in cardiovascular disease (1). A normal VFT implied optimal formation of the transmitral vortex, thus ensuring an effective transfer of circulation impulse energy for efficient blood flow (2). The vortex rings generated from starting jets stop forming and pinched off from the generating jet for sufficiently ventricular filling. The open distance of the mitral valve determined value of VFT following equation (1). In recent years, several studies have shown that VFT reflects the quality of ventricular filling and is correlated with transmitral thrust and mitral annulus recoil, and in particular, transmitral vortex formation has been shown to play an important role in diastolic function (2-4). Therefore, VFT has been considered a useful marker for assessing diastolic performance (5,6).

Cardiovascular magnetic resonance (CMR) has been accepted as the "gold standard" for the assessment of left ventricular (LV) morphology and systolic function, but CMR assessment of LV diastolic function has been limited (7). Four-dimensional flow (4D flow) CMR was developed to provide a comprehensive assessment of blood flow through the heart and large vessels. This unique technique enabled both visualization and quantification of blood flow in the heart (8). Several have authors reported that tricuspid flow and regurgitation can be assessed with good reproducibility and consistency using 4D flow CMR and echocardiography (9). Automated 4D flow analysis has improved the accuracy of peak mitral inflow velocity measurements and enabled tracking of the mitral valve plane motion (10). These studies provided the basis of evaluating VFT by 4D flow CMR.

Tetralogy of Fallot (TOF) is the most common cyanotic congenital heart disease. Early surgical intervention has improved survival rates of TOF patients, but complications such as pulmonary regurgitation (PR), right ventricle hypertrophy, and structural myocardial changes have continued to occur (11,12). To the best of our knowledge, the VFT assessment of diastolic function using 4D flow CMR has not been used in repair of TOF (rTOF) (1). Our previous study highlighted the importance of vortical blood flow patterns for kinetic energy preservation in right ventricle of rTOF patients (13). This was the first study for evaluating LV diastolic dysfunction by VFT measurements using 4D flow CMR in healthy children and rTOF patients. Thus, the aims of this study were to (I) establish reference ranges for VFT measurements in healthy children and adolescents using 4D flow CMR imaging; and (II) analyze VFT parameters to assess diastole dysfunction in a rTOF patient group. We present the following article in accordance with the MDAR reporting checklist (available at https://tp.amegroups.com/article/view/10.21037/tp-22-67/rc).

Methods

Participants

We acquired CMR datasets of 62 healthy Chinese children and adolescents (aged 6–18 years; male: 40; female: 22) and 20 patients with rTOF (aged 10–13 years; male: 15, female: 5) from studies performed between June 2017 and April 2021. We recruited 6–18 years old participants by the network platform (https://h.eqxiu.com/s/Mgzk8jcR?eqrcode=1&from=singlemessage&share_level=1&from_user=2022032551a044a1&from_id=61704003-9&share_time=1648518974336). All volunteers were healthy children who had normal blood pressure and were free of cardiovascular disease as determined by echocardiography. Children with a family history of any other form of heart disease and obesity were excluded. The study was conducted in accordance with the Declaration of Helsinki (as revised in 2013). The study was approved by research ethics committee board of Shanghai Children's Medical Center (No. SCMCIRB-K2017062). Informed consent was taken from all the participants' guardians. The study sample median age was 13.55 years, encompassing 3 different age groups: (Group 1, 6–under 10 years old, 18 cases; Group 2, over 10–under 14 years old: 30 cases; Group 3, 14–18 years old: 14 cases). The data of healthy controls were acquired without contrast-medium administration.

The inclusion criteria for 20 patients with rTOF were as follows: (I) surgery by pulmonary transannular patching; (II) diagnosis of impaired diastolic function (grade 1 or grade 2) according to the criteria described in the 2016 American Society of Echocardiography guidelines (14); (III) patients

with mild-moderate right ventricular (RV) dilation [RV end-diastolic volume (EDV) index <150 mL/m^2] and significant PR (>20%); and (IV) LV diastolic dysfunction [early and/or late peak diastolic mitral inflow velocity (E/A) <1 or early peak mitral inflow velocity and/or mean mitral annular peak early diastolic velocity (E/E') >13]. The exclusion criteria were as follows: rTOF patients with mitral regurgitation or left atrial enlargement (left atrial maximum volume index >34 mL/m^2).

Intravenous bolus injection of 0.1 mmol/kg gadopentetate dimeglumine was administered to rTOF patients within 15–20 minutes before 4D-flow imaging.

CMR imaging

We conducted CMR on a 3.0 Tesla scanner (Discovery MR 750, GE, Chicago, IL, USA) using an 8-channel phased-array cardiac coil. Whole heart 4D flow CMR was performed [spatial resolution =(1.2–1.8)×(1.2–1.8)×(1.2–1.8) mm^3, field of view (FOV) =340–420 mm^2, slab thickness =60–85 mm, temporal resolution =18.2–34.4 ms, echo time (TE) =2.1 ms, repetition time (TR) =4.3 ms, flip angle =8–12°, bandwidth =62.5 Hz/pixel, and velocity sensitivity =120–160 cm/s] with acquisition volume covering the entire heart. The scan time was 6–8 minutes. We followed the parameter settings of protocol according to 4D flow CMR consensus statement (8). Due to the smaller FOV, higher spatial resolution was recommended in a pediatric population. Retrospective electrocardiogram (ECG)-gating was used and 20–30 cardiac phases were reconstructed to represent 1 average heartbeat. Free breathing was allowed and no respiratory motion compensation was used. We also acquired 2-, 3-, 4-chamber, and short-axis cine two-dimensional balanced steady state free precession (2D b-SSFP) images using standard clinical protocols.

Image post-processing analysis

2D velocity vector field visualization

The 4D flow data from the 62 volunteers were used for 2D velocity vector field visualization in LV outflow tract view using pre-process software (MASS Version 30 March 2020; Leiden University Medical Center, Leiden, The Netherlands) (*Figure 1*).

We used 2 different strategies for assessment of VFT. The first strategy (Strategy 1) was based on ventricular volume measurements performed using the 2D cine b-SSFP CMR data. The second strategy (Strategy 2) used 4D flow CMR data for calculation of the VFT (15).

Strategy 1

The VFT was calculated by the following equation:

$$VFT_{volume} = \frac{4}{\pi} \cdot \alpha^3 \cdot EF \cdot \frac{EWV}{SV} = \frac{4}{\pi} \cdot \frac{EWV}{D^3} \quad [1]$$

where, α was defined as:

$$\alpha = \frac{EDV^{1/3}}{D} \quad [2]$$

with the open distance of the mitral valve, D, calculated as the mean of the maximum distance between the leaflet tips during the rapid filling phase, perpendicular to the flow direction, in the three-chamber view, and the distance between the commissures on a short-axis slice through the mitral valve (*Figure 2*). The E-wave volume (EWV) was defined as the difference in volumes of the LV at the end of the E-wave and ESV.

Strategy 2

The trans-mitral valve velocities and time to peak of E-wave and A-wave were determined from the 4D flow CMR data by semi-automatic segmentation using commercial postprocessing software (Version 5.1; Pie Medical Imaging, Maastricht, The Netherlands) by a single observer with over 3 years of experience in CMR. These measurements were verified by a radiologist with over 20 years of experience in CMR. Excursion of the mitral valve was identified on the LV 2-chamber, 4-chamber 2D cine b-SSFP images. By using the valve-tracking algorithms, measurement planes corrected for aliasing, velocity offset, and through-plane motion were obtained for mitral valve via multiplanar reformatting (*Figure 3*). Once obtained, these planes provided instantaneous velocity and time-averaged velocity measurements within the mitral valve.

The peak filling rate (PFR), EDV, end-systolic volumes (ESV), stroke volume (SV), and ejection fraction (EF) of the LV were determined from short-axis 2D cine b-SSFP images using an automatic segmentation method based on a deep learning algorithm. Papillary muscles and trabeculations were included within the LV blood pool. We assessed ventricular volumes normalized to body surface area (BSA) and Z score based on multivariable models with the square of height, height, weight, and age (16).

We analyzed VFT parameters between age matched subgroup of healthy participants and the rTOF patients group (*Table 1*). Post-processing procedure of vortex ring

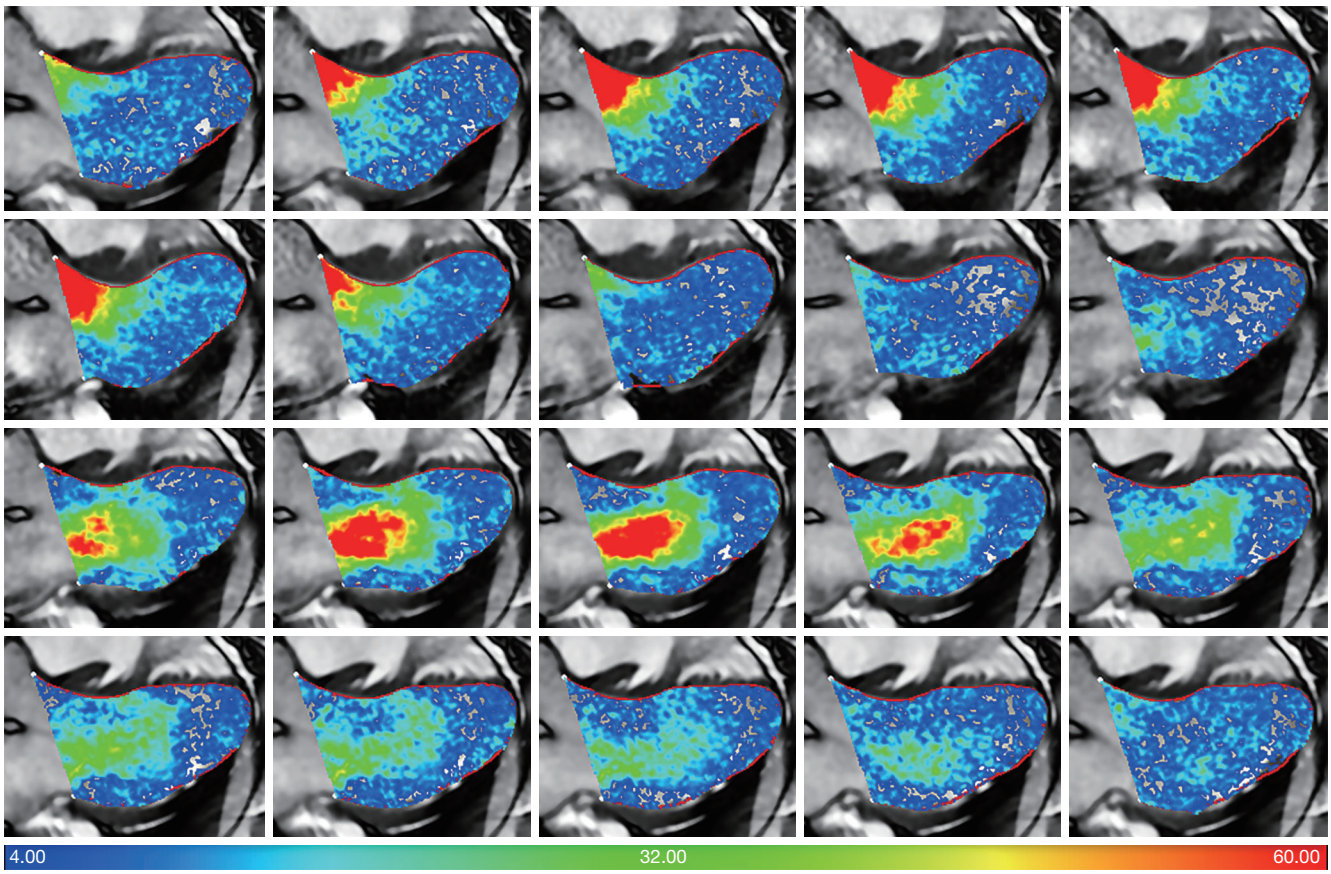

Figure 1 Representative diastolic left ventricular visualizations in control using 4D CMR flow. The color bar represents 2D velocity (cm/s) vector field visualization. CMR, cardiovascular magnetic resonance.

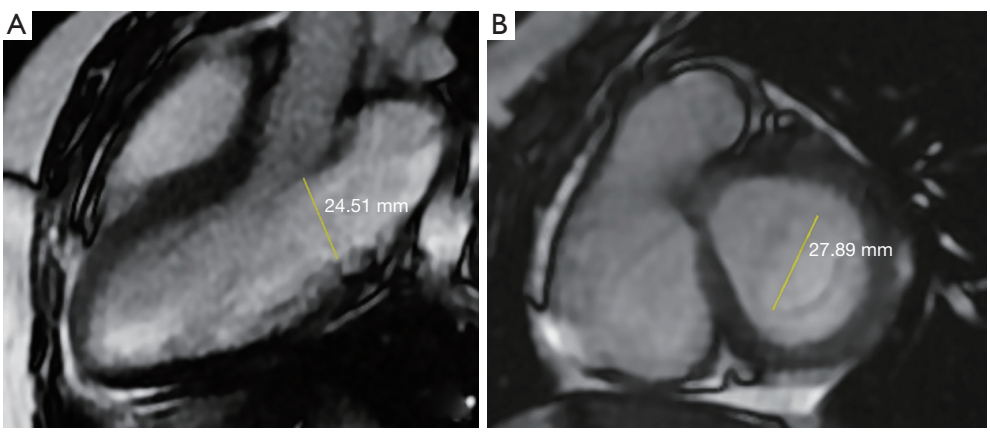

Figure 2 The mitral valve opening distance was calculated by the average of the distance between the commissures seen in the short axis slice (B) of the mitral valve in the 3-chamber view (A), in the rapid filling phase (E wave), perpendicular to the flow direction, the maximum observation distance between the leaflet tips (E wave), and in the short axis slice (B).

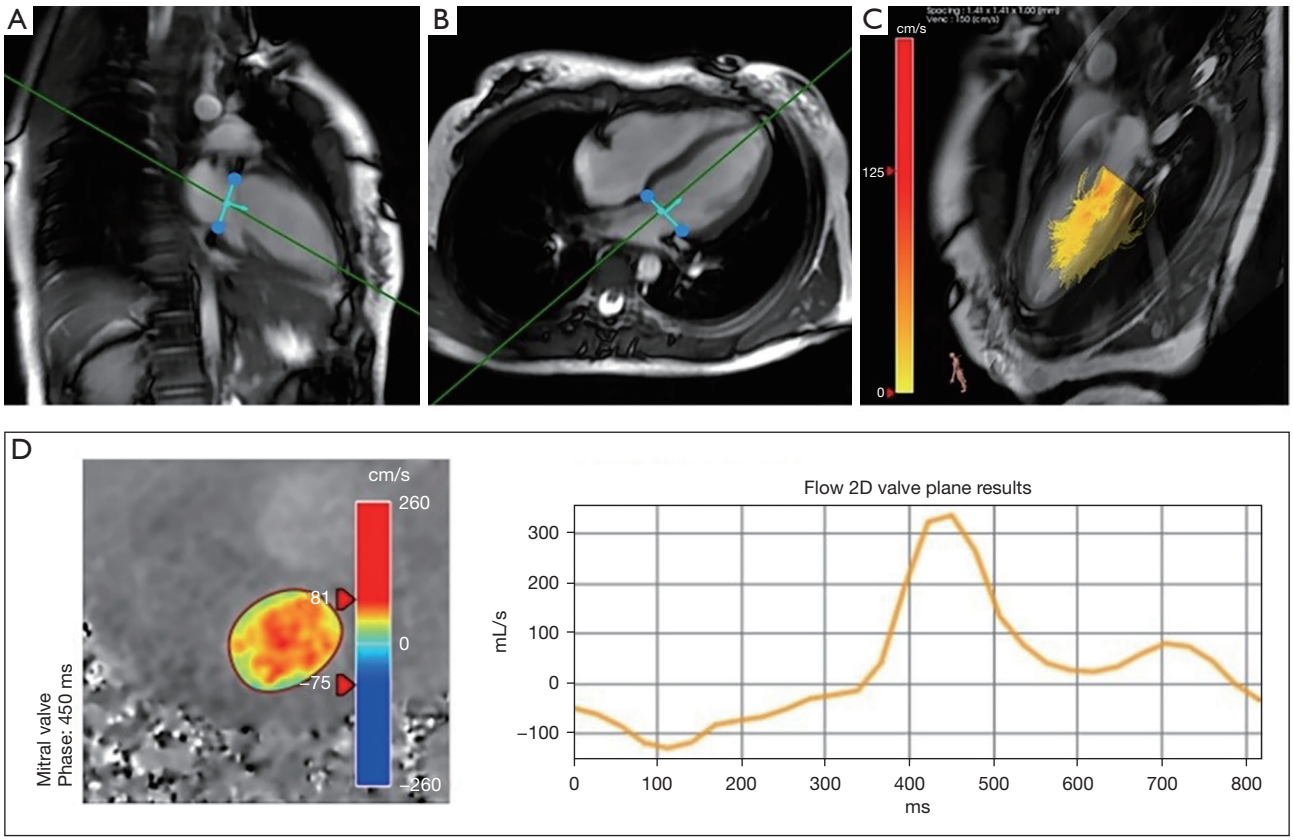

Figure 3 Line graph showing blood flow through the mitral valve during a single cardiac cycle in healthy child volunteer measured using 4D CMR flow sequence. (A) Valve-tracking in two chamber view; (B) valve-tracking in four chamber view; (C) streamline map in the LV; (D) diastolic phase includes early filling, diastole and late filling. CMR, cardiovascular magnetic resonance; LV, left ventricular.

parameters are described in the additional file Figure S1.

Statistical analysis

Statistical analysis was performed using GraphPad Prism version 6.0 (GraphPad Inc., San Diego, CA, USA). Continuous data were reported as mean ± standard deviation. Categorical data were reported as numbers with percentages. We calculated the correlation between VFT and age, heart rate, PFR, time-averaged velocity, and open distance of mitral orifice. Correlation was evaluated using simple linear regression analysis with Pearson r-values calculated for normally distributed data and Spearman r-values for non-normally distributed continuous variables. Correlations were categorized as follows: 0.95–0.80, strong; 0.80–0.60, good; 0.60–0.40, moderate; and less than 0.40, poor. Multiple regression analyses were performed between VFT_{volume} and age, heart rate, PFR, cardiac mass, and VFT_{blood}. A generic linear relationship was calculated between VFT_{volume} and VFT_{blood}. Comparisons among 3 groups were performed using one-way analysis of variance (ANOVA) for normally distributed data and Kruskal-Wallis tests for non-normally distributed continuous variables. Comparison of continuous variables between the rTOF group and volunteer group was performed using an independent-samples *t*-test for normally distributed data, and Mann-Whitney U test for non-normally distributed data. Statistical significance was indicated by $P<0.05$.

Intra-observer and inter-observer reproducibility analysis

The only source of potential observer variability was the user segmentation of the mitral valve. The remaining steps for 2D cine b-SSFP and 4D flow CMR VFT estimations were fully automated. For evaluation of reproducibility, mitral valve segmentation for computation of VFT using the above-mentioned strategies was performed for a sub-group of 20 randomly selected participants, in a random

Table 1 VFT analysis with respect to both their differences between age-matched healthy volunteers and patients

Parameter	rTOF group	Volunteer group	P value
Age (years)	11.85±1.27	12.01±1.27	0.585
N (case)	20	20	
Gender (male/female)	15/5	11/9	
Heart rate (beat/min)	76±11	75±13	0.823
LV EDV indexed to BSA (mL/m^2)	85.18±22.13	80.08±12.19	0.499
LV ESV indexed to BSA (mL/m^2)	35.83±9.16	30.12±6.03	0.026*
LV stroke volume indexed to BSA (mL/m^2)	45.95±6.97	50.27±7.89	0.199
LV EF (%)	57.90±4.96	62.55±4.67	0.004*
VFT_{volume}	5.44±1.93	4.27±0.88	0.018*
VFT_{blood}	3.75±0.81	4.26±0.94	0.078

Data were expressed as mean ± standard deviation. *, statistically significant differences. VFT, vortex formation time; rTOF, repair of tetralogy of Fallot; LV EDV, left ventricular end-diastole volume; BSA, body surface area; LV ESV, left ventricular end-systolic volume; EF, ejection fraction.

order by 2 independent operators (with 3 years' experience in CMR image processing), both blinded to participant's characteristics and quantitative results. Both the open distance of the mitral orifice and VFT measurements for the separate segmentations were compared with calculations of bias, intraclass correlation coefficient (ICC), and coefficient of variation (CoV).

Results

Comparisons between VFT measurements and clinical physiological parameters

Normal mean value of VFT_{volume} and VFT_{blood} were 4.25±0.92 and 3.77±1.11 in healthy child participants. The VFT_{volume} measurements demonstrated good correlation to VFT_{blood} measurements (r=0.61, P<0.001). There was significant correlation between VFT_{volume} and PFR (r=0.46, P<0.001), VFT_{volume} and heart rate (r=-0.25, P=0.04), and VFT_{volume} and LV mass (r=0.32, P=0.01). There was no significant correlation between VFT_{volume} and age (r=0.19, P=0.13), or VFT_{volume} and time-averaged velocity of mitral orifice (r=0.17, P=0.18). There were moderate but significant correlations between VFT_{blood} and PFR (r=0.47, P<0.001), VFT_{blood} and age (r=0.41, P=0.002), and VFT_{blood} and LV mass (r=0.48, P<0.001). There was no significant correlation between VFT_{blood} and heart rate (r=−0.23, P=0.06), and VFT_{blood} and time-averaged velocity of MV (r=0.22, P=0.08) (*Figure 4*).

Age-dependence of cardiac function and VFT measurements

The LV EDV, LV ESV, and LV SV were significantly increased with age in the 3 different age groups (P<0.001, *Table 2*). Normalized LV volumes and function by BSA and Z score were not significantly different with age in the 3 different age groups (P>0.05, *Table 2*). The E wave volume (EWV) also significantly increased with age (47.62±11.37 *vs.* 61.51±16.07 *vs.* 67.81±11.67 mL, P<0.001, *Table 2*). The open distance of the mitral orifice significantly increased with age (24.87±2.25 *vs.* 26.32±2.68 *vs.* 27.31±2.27 mm, P<0.05, *Table 2*). The average velocity of the mitral orifice also demonstrated significant differences between the 3 age groups (88.32±26.69 *vs.* 110.95±34.46 *vs.* 114.44±23.51 cm/s, P<0.05, *Table 2*). The VFT_{volume} measurements were not significantly different between the age groups (3.96±0.77 *vs.* 4.34±1.02 *vs.* 4.32±0.99, P>0.05). However, VFT_{blood} measurements were significantly different between the 3 groups (3.23±0.84 *vs.* 3.93±1.24 *vs.* 4.15±0.95, P<0.05) (*Figure 5*). The relationship was calculated between age and VFT by 2 methods (*Figure 6*). Multiple regression analyses demonstrated that VFT_{volume} was independently associated with PFR (T=2.239; P<0.05) and VFT_{blood} (T=4.361; P<0.001) in *Table 3*. A generic linear relationship was calculated between VFT_{volume} and VFT_{blood} (VFT_{volume} =0.49 VFT_{blood} +3.39, P<0.001) (*Figure 7*).

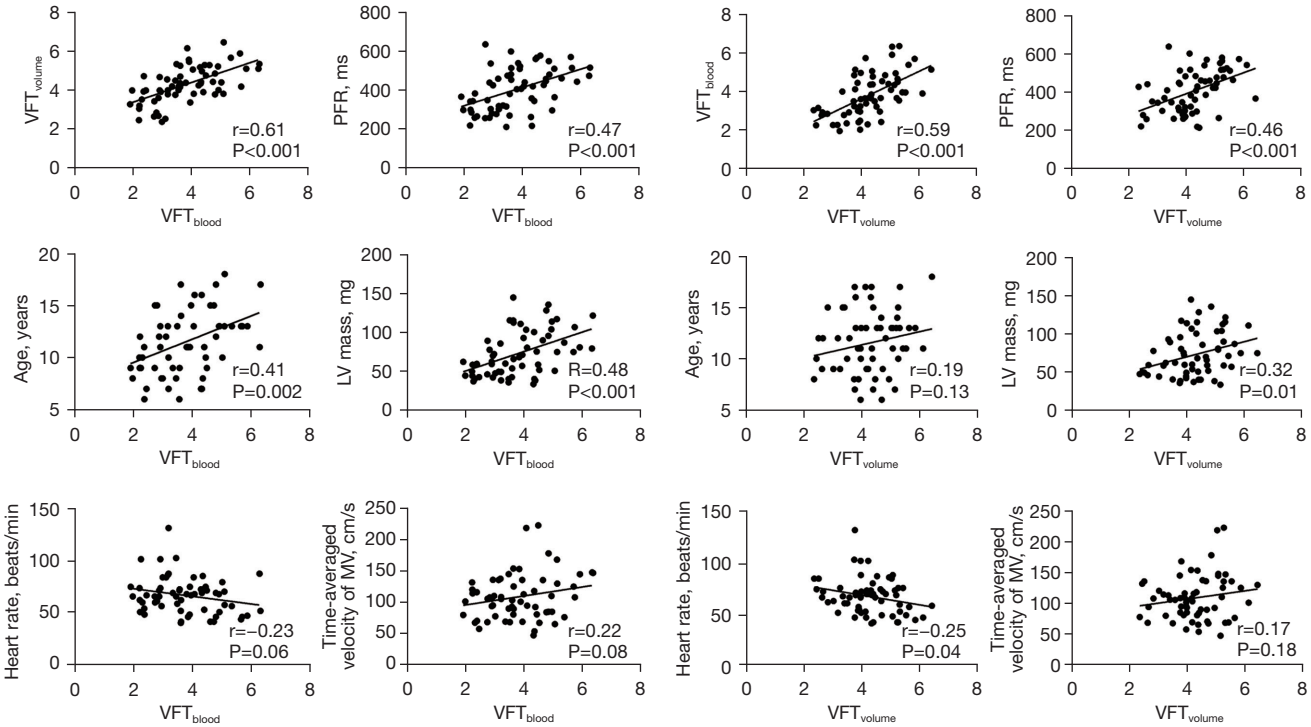

Figure 4 Comparisons between VFT measurements and clinical physiological parameters. VFT, vortex formation time; PFR, peak filling rate; MV, mitral valve; LV, left ventricular.

VFT and MV vortex ring parameters in healthy and rTOF participants

Both LV end systolic volume index (ESVi) and LV EF were significantly different with age among healthy controls and patients with rTOF (P<0.05). The VFT_{volume} was significantly different between healthy controls and patients with rTOF (5.44±1.93 *vs.* 4.27±0.88, P=0.018). The VFT_{blood} was not significantly different between healthy controls and patients with rTOF (3.75±0.81 *vs.* 4.26±0.94, P>0.05, *Table 1*). The VFT_{volume} was significantly correlated with LV EDVi, LV ESV, and cardiac mass in the rTOF patients group (P>0.05, *Table 4*).

The maximal vorticity of LV blood flow in the rTOF patient group was larger than that in the healthy volunteer group during E wave phase (29.3 *vs.* 25.9 s^{-1}). The average vorticity of LV blood flow in the patient group was less than that in the volunteer group during E wave phase (11.7 *vs.* 14.9 s^{-1}). The maximal vorticity of LV blood flow in the patient group was less than in the volunteer group during A wave phase (10.7 *vs.* 12.2 s^{-1}). The average vorticity of LV blood flow in the patient group was less than in the volunteer group during A wave phase (2.1 *vs.* 2.3 s^{-1}) (Figure S1 in supplementary material).

Reproducibility

Table 5 summarizes the results of the intra-observer and inter-observer analysis for mitral orifice open distance and VFT measurements. Intra-observer and inter-observer agreement were excellent for VFT_{volume}, VFT_{blood} and open distance of mitral orifice (all ICCs >96%, CoV <5.3 for intra-observer variability; all ICCs >88%, CoV <11.56 for inter-observer variability).

Discussion

To the best of our knowledge, this was the first study to evaluate VFT measurements of mitral valve flow using 4D flow CMR in healthy children and rTOF patients. Previous investigators had highlighted the importance of vortical blood flow patterns for kinetic energy preservation (2). Other researchers (11,17) had reported 4D flow CMR for quantitative analysis of the LV vortex ring during early and late ventricular filling. We found LV vortex flow during

Table 2 Cardiac physiology and VFT measurements

Parameter	Group 1	Group 2	Group 3	P value
Age (years)	6–9	10–13	14–18	
N (case)	18	30	14	
Gender (male/female)	15/3	14/16	9/5	
Heart rate (beat/min)	86±17	78±13	67±10	0.001*
Body surface area (m^2)	1.08±0.20	1.39±0.19	1.65±0.94	<0.001*
LV EDV (mL/m^2)	80.16±14.55	106.36±23.54	126.81±20.35	<0.001*
LV ESV (mL/m^2)	30.47±8.27	39.63±10.18	51.58±12.73	<0.001*
LV stroke volume (mL/m^2)	49.92±9.59	67.09±16.55	75.22±10.03	<0.001*
LV EDV indexed to BSA (mL/m^2)	76.65±10.45	76.51±13.01	76.75±10.32	0.997
LV ESV indexed to BSA (mL/m^2)	28.25±6.23	28.54±6.34	31.09±6.55	0.388
LV stroke volume indexed to BSA (mL/m^2)	48.38±5.88	48.16±9.45	45.65±5.94	0.554
LV EDV indexed to Z score (mL/m^2)	74.82±10.93	76.48±12.99	76.75±10.41	0.869
LV ESV indexed to Z score (mL/m^2)	28.26±6.23	28.54±6.33	31.09±6.57	0.391
LV stroke volume indexed to Z score (mL/m^2)	46.71±7.46	48.16±9.43	45.65±5.99	0.619
LV EF (%)	63.45±4.65	62.68±6.06	59.71±4.82	0.136
Open distance of mitral orifice (mm)	24.87±2.25	26.32±2.68	27.31±2.27	0.02*
Average velocity of mitral inflow (cm/s)	88.32±26.69	110.95±34.46	114.44±23.51	0.01*
EWV (mL)	47.62±11.37	61.51±16.07	67.81±11.67	<0.001*
VFT_{volume}	3.96±0.77	4.34±1.02	4.32±0.99	0.19
VFT_{blood}	3.23±0.84	3.93±1.24	4.15±0.95	0.03*

Data were expressed as mean ± standard deviation. *, statistically significant differences denoted. Group 1: 6–9 years; Group 2: 10–13 years; Group 3: 14–18 years. VFT, vortex formation time; LV EDV, left ventricular end-diastole volume; LV ESV, left ventricular end-systolic volume; BSA, body surface area; EF, ejection fraction; EWV, E wave volume.

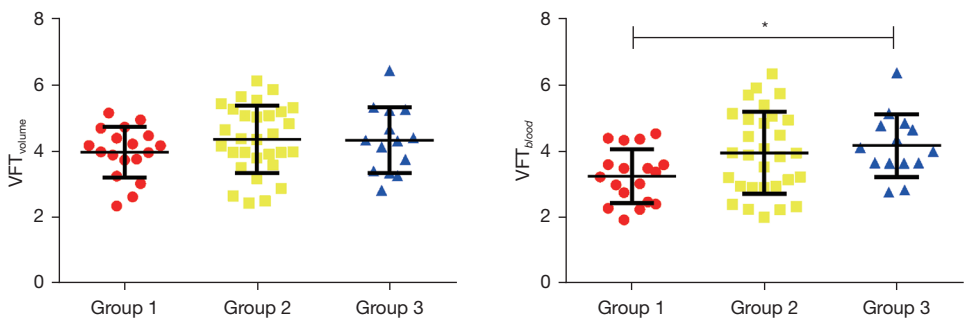

Figure 5 VFT measurements performed with volume (A) and blood flow (B) based measurement strategies for each of the 3 different age groups (Group 1: 6–9 years; Group 2: 10–13 years; Group 3: 14–18 years). *, indicates statically significant difference between VFT_{blood} measurements. VFT, vortex formation time.

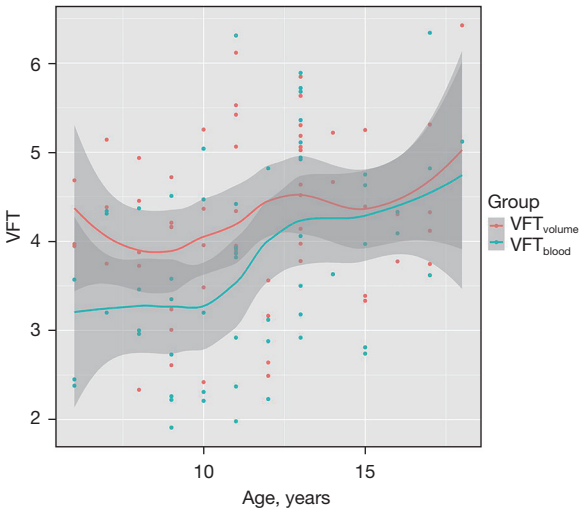

Figure 6 The relationship between age and vortex formation time by 2 methods including 95% CI. VFT, vortex formation time; CI, confidence interval.

Table 3 Multiple regression analyses of VFT and left cardiac function in healthy participants

Parameter	VFT_{volume}	
	T value	P value
Age	−1.217	0.228
Heart rate	−1.157	0.252
Peak filling rate	2.239	0.03*
Cardiac mass	−0.377	0.708
VFT_{blood}	4.361	<0.001*

*, statistically significant differences. VFT, vortex formation time.

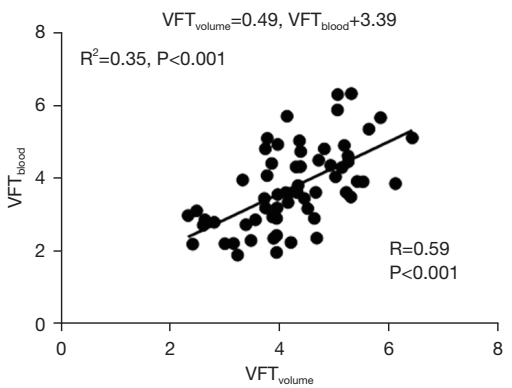

Figure 7 A generic linear relationship (VFT_{volume} and VFT_{blood}) indicated by the solid black line. VFT, vortex formation time.

early and late ventricular filling in rTOF patients and control subjects can be imaging by 4D CMR flow and be visualized using postprocessing in software. In our study, VFT_{volume} and VFT_{blood} were calculated based upon CMR to offer the additional potential intracardiac markers (8).

VFT as index of diastolic function

Pinched-off vortex rings have been shown to be optimal for efficient blood flow within the LV and contribute to the distribution of flow-related stress loads. Previous studies had shown that vortex formation time could be affected by (I) time-dependent velocity of the fluid flow; (II) the Reynolds number of flow (18); and (III) the shape of the mitral orifice (19). In our study, VFT_{blood} was calculated based on an equation that included the above factors. The VFT_{blood} was found to be positively correlated with VFT_{volume} measured based upon ventricular volume measurements. This positive correlation between VFT_{volume} and VFT_{blood} strongly supported the robustness of VFT measurement. We detected a generic linear relationship, as indicated by the solid black line in *Figure* 7. This formula was helpful to correct the variability of VFT_{blood}. In a previous study, Kovács *et al.* (20) demonstrated that vortex formation was causally connected to rapid filling, which is a known consequence of overall diastolic function characterized by load, relaxation, and stiffness. The PFR was determined from ventricular time-volume curves obtained from CMR imaging and could be calculated as an indicator of diastolic function (21). In our study, multiple regression analyses demonstrated that VFT_{volume} was independently associated with PFR and VFT_{blood}, respectively. At present, the clinical significance of markers as surrogate is unknown for ventricular diastolic function and blood flow momentum (22). Matsuura *et al.* demonstrated the close relationship between vortex and intraventricular pressure difference and showed both of them can become new markers of the left ventricular relaxation property (23). Further research is needed to better understand intracardiac flow mechanisms, particularly in children and adolescents.

VFTvolume and VFTblood in children and adolescents

Gharib *et al.* measured the VFT for healthy adults (>20 years old) and found an optimal value of VFT in a narrow range between 3.5 and 5.5. A negative correlation between age and VFT was shown in their

Table 4 The correlation of VFT and left cardiac function in rTOF patients

LV function	VFT_{volume}		VFT_{blood}	
	r value	P value	r value	P value
LV EDV indexed to BSA (mL/m^2)	0.546	0.012*	0.087	0.714
LV ESV indexed to BSA (mL/m^2)	0.595	0.005*	–0.027	0.911
LV stroke volume indexed to BSA (mL/m^2)	0.106	0.657	0.378	0.101
LV cardiac mass (g)	0.685	0.002*	–0.172	0.468

*, statistical differences. VFT, vortex formation time; rTOF, repair of tetralogy of Fallot; LV EDV, left ventricular end-diastole volume; BSA, body surface area; LV ESV, left ventricular end-systolic volume.

Table 5 Intra-observer and inter-observer variability for mitral orifice open distance and VFT measurements

Parameter	Intra-observer (n=20)			Inter-observer (n=20)		
	Bias (limits of agreement)	ICC	CoV	Bias (limits of agreement)	ICC	CoV
Mitral orifice open distance (mm)	0.17 (–0.91 to 1.26)	98.5%	2.21	0.33 (–1.15 to 1.81)	97.3%	3.15
VFT_{volume}	–0.11 (–0.55 to 0.33)	96.8%	5.29	–0.03 (–0.69 to 0.63)	93%	7.56
VFT_{blood}	0.11 (–0.26 to 0.47)	97.4%	5.30	0.19 (–0.56 to 0.93)	88.9%	11.56

VFT, vortex formation time; ICC, intraclass correlation coefficient; CoV, coefficient of variation.

measurements (1). Previous studies reported that age was associated with a reduction in LV filling efficiency quantified using VFT, and adverse or negative correlation was found between age and VFT using linear regression analysis (24-26). Based on this negative correlation, it could be speculated that the value of VFT should be between 6 and 8 for teenagers. However, our results were inconsistent with latter speculation. In our study, VFT_{volume} did not exhibit significant differences between age groups and VFT_{volume} approached the previously determined optimal VFT of 4.0. Nonetheless, our findings might be consistent with known processes of growth given that the reduction of the intraventricular pressure gradients occurs at the same time as the increase of mitral valve area (27). In theory, the vortex rings in the LV of teenagers should still satisfy the optimal principle of VFT with these vortex rings optimized for efficient fluid transport. Our findings based upon VFT_{volume} also suggested that the LV had appropriate space to form the optimal vortex ring in normal children and adolescents from 6 to 18 years old.

By using VFT_{blood} obtained by 4D flow CMR, the volunteer cohort data showed that VFT_{blood} was in optimal range for Group 2 and Group 3, but below the previously determined optimal range in Group 1. This phenomenon might imply that the blood transport in the LV for older children (>10 years old) was more efficient than for younger children (<10 years old). Our results suggested that the normal mean values of VFT_{Volume} and VFT_{blood} in children are lower than the adults' normal range. Kulkarni *et al.* (28) indicated that VFT was attenuated in neonates and infants and increased to the adults' normal range by adolescence. Their explanation was that in children (<10 years old) LV has a low peak torsion, untwisting velocity, smaller dimensions, and faster heart rates compared to adults. In our study, VFT_{volume} measurements were not significantly different between the age groups. Our results deviated from the literature due to the lack of neonates and infants, and further study is required. To sum up, the results from calculation of VFT_{volume} and VFT_{blood} presented that the value of vortex rings in the LV for children over 10 years old were consistent with previous determined unified optimal formation number (VFT ≈4).

Clinical applications of VFTvolume and VFTblood in rTOF

Previous studies have reported that peak systolic LV kinetic energy was decreased in rTOF patients. Unlike

systolic kinetic energy, VFT is a more sensitive indicator for assessment of diastolic function (29). The abnormal flow has been associated with increased viscous energy loss and reduced LV function in pediatric TOF patients (30). We also quantified VFT in a pilot application in controls with rTOF patients. The VFT_{volume} of participants was statistically significant compared with the aged-matched subgroup of controls. We explained that right ventricular dilation leads to left ventricular diastolic insufficiency, the trans-mitral jet velocity was disproportionately increased, which leads to higher VFT. Diastolic dysfunction of LV disrupted the interaction between the vortex and ventricular wall. The trans-mitral vortex pinch-off tends to occur in infinity, or alternatively may never occur. In this situation, the blood flow momentum was mainly transferred through the jet that led to high-energy dissipation and incoherent flow structures. Previous investigations have indicated that there are significant reductions in systolic kinetic energy and altered distribution of hemodynamic forces in rTOF patients (31). In our study, VFT_{volume} was significantly correlated with cardiac mass in the rTOF patients group.

Reproducibility of VFTvolume and VFTblood

The ICC and CoV for VFT_{volume}, VFT_{blood} and mitral orifice open distance are summarized in *Table 5* for the intra-observer and inter-observer variability study. Mitral orifice opening distance showed a higher ICC and CoV than VFT_{volume} and VFT_{blood}. However, there was still good reproducibility for both VFT_{volume} and VFT_{blood} in our study.

Limitations

There were some limitations to this study. Firstly, this was a single-center prospective study performed at a large hospital. The inherent limitations of this study design cannot be avoided. Secondly, Rutkowski *et al.* (32) demonstrated a gender-based cardiac efficiency relationship between cardiac function and flow. Gender difference may also be one of the factors affecting VFT, which has not been reported. Our study did not consider the effect of gender upon VFT as a larger cohort would be needed to test this gender difference. Thirdly, the mitral orifice opening distances were determined from CMR data using semi-automatic segmentation. In general, mitral annulus morphology for size and shape was addressed adequately by as few as 6 radial slices (33). We calculated opening distance of the mitral valve only by 3-chamber view and short axis view. Additional studies in the future may be required with direct tracing of the mitral orifice to further improve the accuracy of VFT calculations. Finally, according to our implemented VFT equation, the definition should be mass/energy supply ratio rather than a physical VFT. The total kinetic energy of a vortex ring consisted of not only the translational energy associated with impulse and velocity but also the rotational energy associated with vorticity distribution. Future prospective, large-scale, multicenter investigations are needed to verify the prognostic value of VFT_{volume} in rTOF patients.

Conclusions

The VFT measurements showed that the LV had appropriate space to form the optimal vortex ring in normal children and adolescents aged 6 to 18 years old. The VFT_{volume} could potentially be helpful in improving our understanding of LV diastolic dysfunction in rTOF patients.

Acknowledgments

Funding: This study was supported by grants from the National Key Clinical Specialty Project, the National Natural Science Foundation of China (No. 82171902) and Shanghai Committee of Science and Technology (No. 21Y11910700). This study was supported by Shanghai "Rising Stars of Medical Talent" Medical Imaging Practitioner Program.

Footnote

Reporting Checklist: The authors have completed the MDAR reporting checklist. Available at https://tp.amegroups.com/article/view/10.21037/tp-22-67/rc

Data Sharing Statement: Available at https://tp.amegroups.com/article/view/10.21037/tp-22-67/dss

Conflicts of Interest: All authors have completed the ICMJE uniform disclosure form (available at https://tp.amegroups.com/article/view/10.21037/tp-22-67/coif). All authors report technical assistance from Gaston Vogel and Qiuchen Wang (Pie Medical Imaging Corporation Netherlands), and statistical assistance from Tingfan Wu (GE Healthcare). The authors have no other conflicts of interest to declare.

Ethical Statement: The authors are accountable for all

aspects of the work in ensuring that questions related to the accuracy or integrity of any part of the work are appropriately investigated and resolved. The study was conducted in accordance with the Declaration of Helsinki (as revised in 2013). The study was approved by research ethics committee board of Shanghai Children's Medical Center (No. SCMCIRB-K2017062). Informed consent was taken from all the participants' guardians.

References

1. Gharib M, Rambod E, Kheradvar A, et al. Optimal vortex formation as an index of cardiac health. Proc Natl Acad Sci U S A 2006;103:6305-8.
2. Kheradvar A, Assadi R, Falahatpisheh A, et al. Assessment of transmitral vortex formation in patients with diastolic dysfunction. J Am Soc Echocardiogr 2012;25:220-7.
3. Poh KK, Lee LC, Shen L, et al. Left ventricular fluid dynamics in heart failure: echocardiographic measurement and utilities of vortex formation time. Eur Heart J Cardiovasc Imaging 2012;13:385-93.
4. Pedrizzetti G, Domenichini F. Left ventricular fluid mechanics: the long way from theoretical models to clinical applications. Ann Biomed Eng 2015;43:26-40.
5. Maragiannis D, Alvarez PA, Schutt RC, et al. Vortex Formation Time Index in Patients With Hypertrophic Cardiomyopathy. JACC Cardiovasc Imaging 2016;9:1229-31.
6. Ambhore A, Ngiam JN, Chew NWS, et al. Optimal vortex formation time index in mitral valve stenosis. Int J Cardiovasc Imaging 2021;37:1595-600.
7. Panesar DK, Burch M. Assessment of Diastolic Function in Congenital Heart Disease. Front Cardiovasc Med 2017;4:5.
8. Dyverfeldt P, Bissell M, Barker AJ, et al. 4D flow cardiovascular magnetic resonance consensus statement. J Cardiovasc Magn Reson 2015;17:72.
9. Driessen MMP, Schings MA, Sieswerda GT, et al. Tricuspid flow and regurgitation in congenital heart disease and pulmonary hypertension: comparison of 4D flow cardiovascular magnetic resonance and echocardiography. J Cardiovasc Magn Reson 2018;20:5.
10. Feneis JF, Kyubwa E, Atianzar K, et al. 4D flow MRI quantification of mitral and tricuspid regurgitation: Reproducibility and consistency relative to conventional MRI. J Magn Reson Imaging 2018;48:1147-58.
11. Gatzoulis MA, Balaji S, Webber SA, et al. Risk factors for arrhythmia and sudden cardiac death late after repair of tetralogy of Fallot: a multicentre study. Lancet 2000;356:975-81.
12. Wang SY, OuYang RZ, Hu LW, et al. Right and left ventricular interactions, strain, and remodeling in repaired pulmonary stenosis patients with preserved right ventricular ejection fraction: A cardiac magnetic resonance study. J Magn Reson Imaging 2020;52:129-38.
13. Zhao X, Hu L, Leng S, et al. Ventricular flow analysis and its association with exertional capacity in repaired tetralogy of Fallot: 4D flow cardiovascular magnetic resonance study. J Cardiovasc Magn Reson 2022;24:4.
14. Nagueh SF, Smiseth OA, Appleton CP, et al. Recommendations for the Evaluation of Left Ventricular Diastolic Function by Echocardiography: An Update from the American Society of Echocardiography and the European Association of Cardiovascular Imaging. Eur Heart J Cardiovasc Imaging 2016;17:1321-60.
15. Dabiri JO. Optimal Vortex Formation as a Unifying Principle in Biological Propulsion. Annu Rev Fluid Mech 2009;41:17-33.
16. Cardinal MP, Blais S, Dumas A, et al. Novel Z Scores to Correct Biases Due to Ventricular Volume Indexing to Body Surface Area in Adolescents and Young Adults. Can J Cardiol 2021;37:417-24.
17. Töger J, Kanski M, Arvidsson PM, et al. Vortex-ring mixing as a measure of diastolic function of the human heart: Phantom validation and initial observations in healthy volunteers and patients with heart failure. J Magn Reson Imaging 2016;43:1386-97.
18. Gao L, Yu SCM. Development of the trailing shear layer in a starting jet during pinch-off. J Fluid Mech 2012;700:382-405.
19. Dabiri JO, Gharib M. Starting flow through nozzles with temporally variable exit diameter. J Fluid Mech 2005;538:111-36.
20. Kovács SJ, McQueen DM, Peskin CS. Modelling cardiac fluid dynamics and diastolic function. Philosophical Transactions: Mathematical, Physical and Engineering

Sciences 2001;359:1299-314.
21. Göransson C, Vejlstrup N, Carlsen J. Reproducibility of peak filling and peak emptying rate determined by cardiovascular magnetic resonance imaging for assessment of biventricular systolic and diastolic dysfunction in patients with pulmonary arterial hypertension. Int J Cardiovasc Imaging 2018;34:777-86.
22. Kheradvar A, Rickers C, Morisawa D, et al. Diagnostic and prognostic significance of cardiovascular vortex formation. J Cardiol 2019;74:403-11.
23. Matsuura K, Shiraishi K, Sato K, et al. Left ventricular vortex and intraventricular pressure difference in dogs under various loading conditions. Am J Physiol Heart Circ Physiol 2019;316:H882-H888.
24. Sengupta PP, Narula J, Chandrashekhar Y. The dynamic vortex of a beating heart: wring out the old and ring in the new! J Am Coll Cardiol 2014;64:1722-4.
25. Pedrizzetti G, La Canna G, Alfieri O, et al. The vortex--an early predictor of cardiovascular outcome? Nat Rev Cardiol 2014;11:545-53.
26. Pagel PS, Dye L 3rd, Boettcher BT, et al. Advanced Age Attenuates Left Ventricular Filling Efficiency Quantified Using Vortex Formation Time: A Study of Octogenarians With Normal Left Ventricular Systolic Function Undergoing Coronary Artery Surgery. J Cardiothorac Vasc Anesth 2018;32:1775-9.
27. Krueger PS, Gharib M. The significance of vortex ring formation to the impulse and thrust of a starting jet. Physics of Fluids 2003;15:1271-81.
28. Kulkarni A, Morisawa D, Gonzalez D, et al. Age-related changes in diastolic function in children: Echocardiographic association with vortex formation time. Echocardiography 2019;36:1869-75.
29. Sjöberg P, Bidhult S, Bock J, et al. Disturbed left and right ventricular kinetic energy in patients with repaired tetralogy of Fallot: pathophysiological insights using 4D-flow MRI. Eur Radiol 2018;28:4066-76.
30. Schäfer M, Barker AJ, Jaggers J, et al. Abnormal aortic flow conduction is associated with increased viscous energy loss in patients with repaired tetralogy of Fallot. Eur J Cardiothorac Surg 2020;57:588-95.
31. Sjöberg P, Töger J, Hedström E, et al. Altered biventricular hemodynamic forces in patients with repaired tetralogy of Fallot and right ventricular volume overload because of pulmonary regurgitation. Am J Physiol Heart Circ Physiol 2018;315:H1691-702.
32. Rutkowski DR, Barton GP, François CJ, et al. Sex Differences in Cardiac Flow Dynamics of Healthy Volunteers. Radiol Cardiothorac Imaging 2020;2:e190058.
33. Leng S, Zhang S, Jiang M, et al. Imaging 4D morphology and dynamics of mitral annulus in humans using cardiac cine MR feature tracking. Sci Rep 2018;8:81.

(English Language Editor: J. Jones)

Cite this article as: Hu LW, Xiang Y, Qin SY, Ouyang RZ, Liu JL, Peng YF, Xie WH, Zhang Y, Liu H, Zhong YM. Vortex formation time as an index of left ventricular filling efficiency: comparison between children volunteers and patients with tetralogy of Fallot. Transl Pediatr 2022;11(6):869-881. doi: 10.21037/tp-22-67

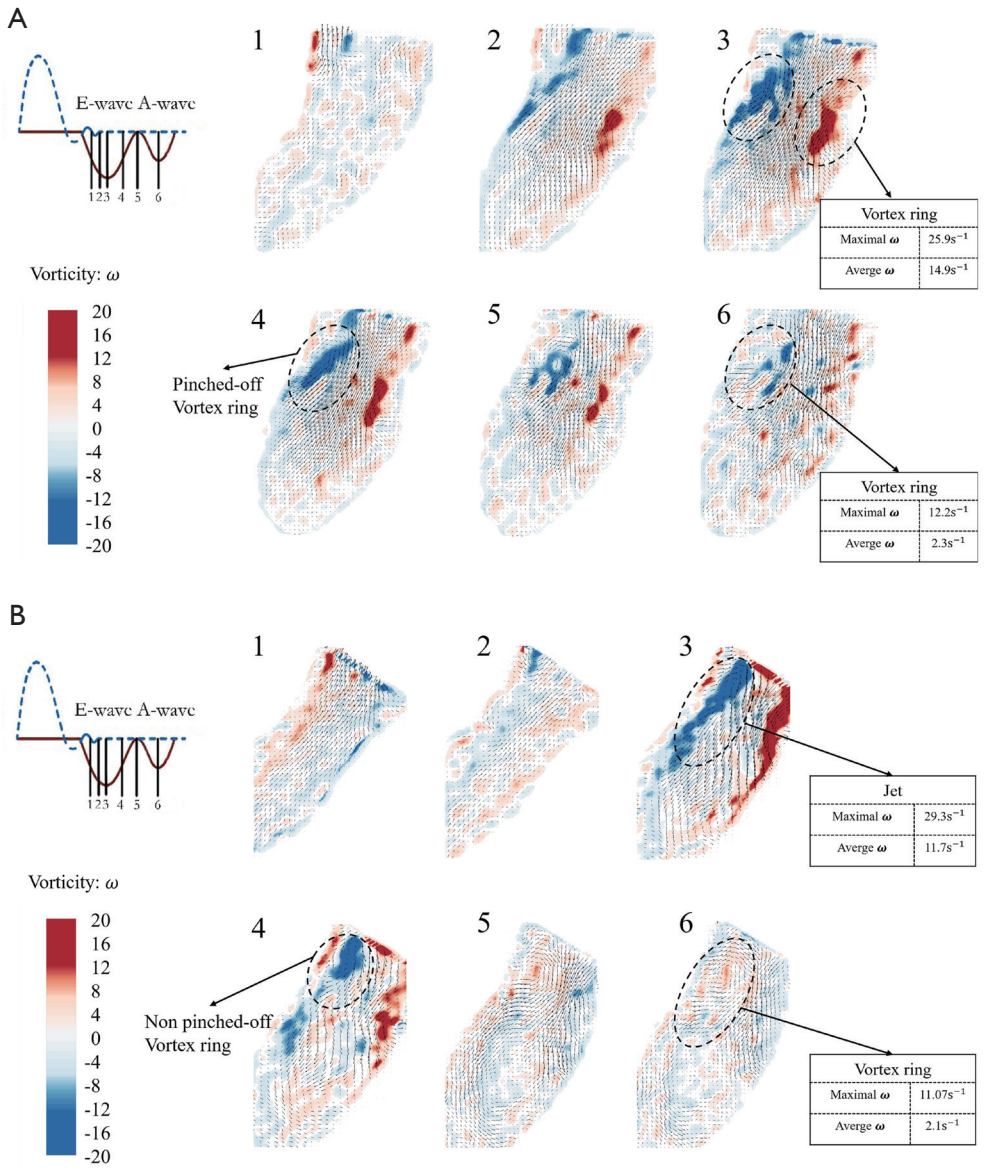

Figure S1 Velocity vector superimposed with vorticity contour of the LV blood flow for a rTOF patient case (A) and a volunteer case (B) during a diastole. The times denoted by 3 and 6 indicate the peak E-wave and the peak A-wave, respectively. In *Figure* 7, the evolution of the LV blood flow for a healthy volunteer and a rTOF patient was shown. For the healthy volunteer, a vortex ring structure appeared at the peak E-wave and then pinched off during E-wave deceleration. However, a jet-like flow was generated at the peak E-wave for the rTOF patient and a non-pinched-off vortex ring rolled up during E-wave deceleration. The underlying reason was the insufficiency of LV diastolic function of the rTOF patient, which caused there was no enough space for vortex ring formation. VFTvolume of the rTOF patient group was larger than that of the healthy volunteer's group. It is undoubted that the velocity of jet-like blood flow was larger than that of vortex-ring blood flow, resulting in the maximal vorticity of LV blood flow during E wave phase in rTOF case was larger than that for healthy volunteer. However, the average vorticity of LV blood flow in rTOF case was less than in volunteer case during E wave phase (11.7 s^{-1} *vs.* 14.9 s^{-1}). This suggests that the total energy of LV blood in rTOF case is less than that in volunteer case.

https://dx.doi.org/10.21037/tp-22-67